Hearing the Triangles: A Numerical Perspective

Wei Gong[1], Xiaodong Liu[1,*] and Jing Wang[2]

[1] *Academy of Mathematics and Systems Science, Chinese Academy of Sciences, Beijing 100190, P.R. China.*
[2] *School of Mathematical Sciences, University of Chinese Academy of Sciences, Beijing 100049, P.R. China.*

Abstract. We introduce a two-step numerical scheme for reconstructing the shape of a triangle by its Dirichlet spectrum. With the help of the asymptotic behavior of the heat trace, the first step is to determine the area, the perimeter, and the sum of the reciprocals of the angles of the triangle. The shape is then reconstructed, in the second step, by an application of the Newton's iterative method or the Levenberg-Marquardt algorithm for solving a nonlinear system of equations on the angles. Numerically, we have used only finitely many eigenvalues to reconstruct the triangles. To our best knowledge, this is the first numerical simulation for the classical inverse spectrum problem in the plane. In addition, we give a counter example to show that, even if we have infinitely many eigenvalues, the shape of a quadrilateral may not be heard.

1   Introduction

Since the landmark paper by Marc Kac in 1966 [15], the question "Can one hear the shape of a drum?" has attracted and inspired many mathematicians. This forms the subject of the mathematical discipline called spectral geometry.

More exactly, for a bounded simply connected domain $D \subset \mathbb{R}^2$, the vibration of a drum (membrane) which spans D, is governed by the wave equation

$$v_{tt} - \Delta v = 0,$$

Corresponding author. Email addresses: `wgong@lsec.cc.ac.cn` (W. Gong), `xdliu@amt.ac.cn` (X. Liu), `wangjing226@mails.ucas.ac.cn` (J. Wang)

where $v = v(x,t)$ denotes the displacement in some direction of a point $x \in D$ at time $t > 0$ and the Laplacian Δ is taken with respect to the spatial variables $x = (x_1, x_2)$. Of particular interest are the time harmonic solutions in the form

$$v = e^{i\omega t} u(x),$$

where the spatial part u solves the stationary equation

$$\Delta u + \omega^2 u = 0 \quad \text{in } D \tag{1.1}$$

with the Dirichlet boundary condition

$$u = 0 \quad \text{on } \partial D, \tag{1.2}$$

corresponding to the drum being fixed along its boundary.

We call $\lambda := \omega^2 > 0$ a Dirichlet eigenvalue of D if there is a nontrivial solution $u \neq 0$ of (1.1)-(1.2). For a fixed domain D, it is well known that, if we repeat each eigenvalue according to its (finite) multiplicity, we have

$$0 < \lambda_1 < \lambda_2 \leq \lambda_3 \leq \cdots$$

and

$$\lambda_n \rightarrow \infty \quad \text{as} \quad n \rightarrow \infty.$$

The distribution of the eigenvalues has been thoroughly investigated and a considerable amount of information is available. For survey articles on this subject we refer to [11, 16].

Conversely, we are interested in the inverse problem: Is the domain D determined uniquely by its Dirichlet eigenvalues. In 1992, Gordon *et al.* [10] had constructed two concave polygons which are isospectral, but not congruent. However, it is still open for a general convex polygon or a domain with smooth boundary. We refer to [6, 23] for the uniqueness results if the boundary is analytic with some symmetry. In a recent work, the uniqueness has also been established for ellipses of small eccentricity [14].

This work focuses on a numerical scheme for triangles. There have been some papers giving numerical illustrations on various conjectures on spectral geometry as seen, e.g. [1–3]. However, to our best knowledge, this is the first numerical algorithm for reconstructing the shape of a domain from its spectrum. We would like to remark that although the triangle is very specific and simple, it has recently become apparent that triangles do play an important role in both the shape optimization problems [2, 17] and the spectral properties related to isoperimetric inequalities [1, 21]. The uniqueness is first proved by Durso [7]. It is conjectured by Laugesen and Siudeja [17] that the first three eigenvalues are enough to determine the shape of a triangle. However, this is still open up to now. We refer to [3, 5, 9] for some recent study by knowing just finitely many eigenvalues. Our algorithm is motivated by a recent and simpler proof by Grieser and Maronna [12]. The proof is divided into two steps:

- Determine its area $\mathcal{A}$, its perimeter $\mathcal{P}$, and the sum $\mathcal{R}$ of the reciprocals of its angles from the spectrum.

- Determine its angles by a system of equations involving $\mathcal{A}, \mathcal{P}$, and $\mathcal{R}$.

Finally, we want to remind that the uniqueness of the inverse spectral problem for a general polygon is still largely open. Even for quadrilaterals, the uniqueness has only been proved recently for parallelograms [18] and non-obtuse trapezoids [13]. We construct, in this paper, two quadrilaterals that share infinitely many Dirichlet eigenvalues. In other words, the shape of a quadrilateral may not be heard even we have infinitely many eigenvalues.

2   Numerical scheme for triangles

Recall the heat trace

$$\mathbb{h}(t) := \sum_{m=1}^{\infty} e^{-\lambda_m t}, \quad t > 0.$$

For polygons we have the asymptotic behavior [4, 19]

$$\mathbb{h}(t) = a_{-1} t^{-1} + a_{-1/2} t^{-1/2} + a_0 + \mathcal{O}(e^{-c/t}) \quad \text{as} \quad t \to 0 \tag{2.1}$$

for some constant $c > 0$, where

$$a_{-1} = \frac{\mathcal{A}}{4\pi}, \quad a_{-1/2} = -\frac{\mathcal{P}}{8\sqrt{\pi}} \tag{2.2}$$

and

$$a_0 = \frac{1}{24} \sum_i \left(\frac{\pi}{\alpha_i} - \frac{\alpha_i}{\pi} \right)$$

with the interior angles α_i of the polygon. Note that for a triangle, we have $\sum_i \alpha_i = \pi$, which implies that

$$a_0 = \frac{\pi}{24} \mathcal{R} - \frac{1}{24}, \tag{2.3}$$

where

$$\mathcal{R} := \sum_{i=1}^{3} \frac{1}{\alpha_i}.$$

Consequently, the asymptotic behavior (2.1) implies that the area $\mathcal{A}$, the perimeter $\mathcal{P}$, and the sum $\mathcal{R}$ of the reciprocals of the angles of the triangle can be heard from all the eigenvalues λ_m. Numerically, take

$$0 < t_1 < t_2 < t_3 < \epsilon,$$

where $\epsilon > 0$ is small enough. Taking M large enough, we define

$$\mathbb{h}_M(t) := \sum_{m=1}^{M} e^{-\lambda_m t}, \quad t > 0,$$

$$Y := \left(\mathbb{h}_M(t_1), \mathbb{h}_M(t_2), \mathbb{h}_M(t_3)\right)^T.$$

Then we look for an approximation of $X := (a_{-1}, a_{-1/2}, a_0)^T$ by solving

$$\mathbb{H}X = Y, \tag{2.4}$$

where

$$\mathbb{H} := \begin{pmatrix} t_1^{-1} & t_1^{-1/2} & 1 \\ t_2^{-1} & t_2^{-1/2} & 1 \\ t_3^{-1} & t_3^{-1/2} & 1 \end{pmatrix}$$

is a Vandermonde matrix. Furthermore, we obtain an approximation of $\mathcal{A}, \mathcal{P}$, and $\mathcal{R}$ from (2.2)-(2.3). It is shown that the triangle is determined uniquely up to congruence by the three quantities $\mathcal{A}, \mathcal{P}$, and $\mathcal{R}$ [12]. This follows by verifying that a triple $(\alpha_1, \alpha_2, \alpha_3)$ of positive numbers is uniquely determined, up to ordering, by the equations

$$\alpha_1 + \alpha_2 + \alpha_3 = \pi, \tag{2.5}$$

$$\cot\frac{\alpha_1}{2} + \cot\frac{\alpha_2}{2} + \cot\frac{\alpha_3}{2} = \frac{\mathcal{P}^2}{4\mathcal{A}}, \tag{2.6}$$

$$\frac{1}{\alpha_1} + \frac{1}{\alpha_2} + \frac{1}{\alpha_3} = \mathcal{R}. \tag{2.7}$$

Numerically, we apply Newton's iterative method or the Levenberg-Marquardt algorithm to solve the above nonlinear system of Eqs. (2.5)-(2.7). To do so, we consider a general nonlinear equation

$$F(x) = 0, \tag{2.8}$$

where $x = (x_1, x_2, x_3)^T \in \mathbb{R}^3$ and $F = (F_1, F_2, F_3)$ with $F_i : \mathbb{R}^3 \to \mathbb{R}, i = 1, 2, 3$. We assume that F is differentiable with the Jacobian matrix $J = (\partial_j F_i) : \mathbb{R}^3 \to \mathbb{R}^{3 \times 3}$. Then the standard Newton method reads: Given $x^0 \in \mathbb{R}^3$, perform the iteration

$$x^{n+1} = x^n - J(x^n)^{-1} F(x^n). \tag{2.9}$$

When J is nearly singular around some x, the above Newton iteration does not perform well. In this case, we consider the Levenberg-Marquardt algorithm. Consider the following least-squares problem:

$$\min_{x \in \mathbb{R}^3} \frac{1}{2} \|F(x)\|^2, \tag{2.10}$$

where $\|\cdot\|$ denotes the Euclidean norm for vectors. For given $x^n \in \mathbb{R}^3$, the Levenberg-Marquardt algorithm seeks approximate solution of the following linearized problem:

$$\min_{x \in \mathbb{R}^3} \frac{1}{2} \|F(x^n) + J(x^n)(x - x^n)\|^2 + \frac{\gamma_n}{2} \|x - x^n\|^2, \tag{2.11}$$

which is a regularized version of the standard Gauss-Newton method that seeks solutions of the linearized problem

$$\min_{x \in \mathbb{R}^3} \frac{1}{2} \|F(x^n) + J(x^n)(x - x^n)\|^2. \tag{2.12}$$

In practical applications we need to find an appropriate regularization parameter γ_n. Here we use the choice $\gamma_n = \|F(x^n)\|$ proposed in [8]. Then the Levenberg-Marquardt algorithm reads: Given $x^0 \in \mathbb{R}^3$, perform the iteration

$$x^{n+1} = x^n - \left(\gamma_n I_3 + J(x^n)^T J(x^n)\right)^{-1} J(x^n)^T F(x^n), \tag{2.13}$$

where I_3 is the 3-by-3 identity matrix.

In a sum, we formulate Algorithm 1 for determining the triangles from the corresponding spectrum.

Algorithm 1 Numerical Scheme for Hearing the Triangles.

Step 1. Compute $\mathcal{A}$, $\mathcal{P}$, and $\mathcal{R}$ by solving (2.4).

Step 2. Compute the angles $\{\alpha_1, \alpha_2, \alpha_3\}$ by solving (2.5)-(2.7).

Step 3. Compute the side lengths by

$$\ell_1 = \frac{\mathcal{P} \sin\alpha_1}{\cos\alpha_1 \sin\alpha_2 + \sin\alpha_2 + \sin\alpha_1 \cos\alpha_2 + \sin\alpha_1},$$
$$\ell_2 = \ell_1 \frac{\sin\alpha_2}{\sin\alpha_1},$$
$$\ell_3 = \mathcal{P} - \ell_1 - \ell_2,$$

where $\{\ell_1, \ell_2, \ell_3\}$ denote the lengths of the three sides opposite to $\{\alpha_1, \alpha_2, \alpha_3\}$.

We want to remark that, by using the iterative method, an important issue is the reasonable choice of initial guess. To solve this problem, we introduce a technique for such an initial guess.

Theorem 2.1. *Recall the notations introduced in Fig. 1. For the triangle $\mathcal{T}_{ABC}$, we have an estimate*

$$\frac{4\mathcal{A}}{\mathcal{P}} < h \leq \min\left\{\frac{6\mathcal{A}}{\mathcal{P}}, \frac{\sqrt{3}\mathcal{P}}{4}\right\}.$$
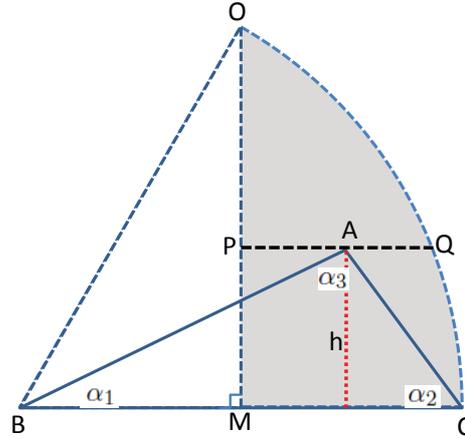
Figure 1: In a sector $\mathcal{S}_{OBC}$ with $BO=BC$ and $\angle OBC=\pi/3$, we introduce a triangle $\mathcal{T}_{ABC}$ with the longest side BC such that the apex A located in the shade domain, where $OM\perp BC$. Denote by h the height with respect to base BC. The line segment PQ passing through the apex A is such that $PQ\parallel BC$ with P located on the line segment OM and Q located on the circular arc OC. The case $A=P$ corresponds to an isosceles triangle such that $AB=AC$, while the case $A=Q$ corresponds to an isosceles triangle such that $BA=BC$.

Proof. By definition of the shade domain in Fig. 1, for the triangle $\mathcal{T}_{ABC}$, we have $AC\leq AB\leq BC$. Therefore,

$$\frac{\mathcal{P}}{3}=\frac{AC+AB+BC}{3}\leq BC<\frac{AC+AB+BC}{2}=\frac{\mathcal{P}}{2}, \tag{2.14}$$

which further implies that

$$\frac{2}{\mathcal{P}}<\frac{1}{BC}\leq\frac{3}{\mathcal{P}}. \tag{2.15}$$

Noting that $\mathcal{A}=hBC/2$, we deduce from (2.15) that

$$\frac{4\mathcal{A}}{\mathcal{P}}<h\leq\frac{6\mathcal{A}}{\mathcal{P}}. \tag{2.16}$$

A straightforward calculation shows that

$$h\leq OM=BO\sin\frac{\pi}{3}=BC\sin\frac{\pi}{3}=\frac{\sqrt{3}}{2}BC.$$

Combining this with (2.14), we have

$$h\leq\frac{\sqrt{3}\mathcal{P}}{4}. \tag{2.17}$$

The proof is finished by (2.16)-(2.17). $\qquad\qquad\square$

Using the estimate in Theorem 2.1, we introduce a simple technique as presented in Algorithm 2 for choosing the initial guess $(\alpha_1,\alpha_2,\alpha_3)$ for the nonlinear system of Eqs. (2.5)-(2.7).

Algorithm 2 A Technique for Choosing the Initial Guess $(\alpha_1, \alpha_2, \alpha_3)$.

- For some integer $M > 1$, we define

$$h_1 := \frac{4\mathcal{A}}{\mathcal{P}},$$

$$\mathbb{h} := \frac{1}{M-1}\left(\min\left\{\frac{6\mathcal{A}}{\mathcal{P}}, \frac{\sqrt{3}\mathcal{P}}{4}\right\} - h_1\right),$$

$$h_m := h_1 + (m-1)\mathbb{h}, \quad m = 1, 2, \dots, M.$$

- Take $B_m C_m = 2\mathcal{A}/h_m$ the basis corresponding to the height $h_m, m = 1, 2, \dots, M$. Consider a sector $\mathcal{S}_{O_m B_m C_m}$ as shown in Fig. 1.

- Divide the line segment $P_m Q_m$ into $N-1$ equal parts for some integer $N > 1$, and take A_n be the n-th collection point, $n = 1, 2, \dots, N$ such that $A_1 = P_m$ and $A_N = Q_m$. Then we construct a triangle $\mathcal{T}_{A_n B_m C_m}$.

- Compute the inner angles $(\alpha_1^{m,n}, \alpha_2^{m,n}, \alpha_3^{m,n})$ from the obtained initial triangle $\mathcal{T}_{A_n B_m C_m}$.

- For each $m = 1, 2, \dots, M, n = 1, 2, \dots, N$, define a residual

$$f_{m,n} := \sqrt{f_1^2 + f_2^2 + f_3^2},$$

  where

$$f_1 := \alpha_1^{m,n} + \alpha_2^{m,n} + \alpha_3^{m,n} - \pi,$$

$$f_2 := \cot\frac{\alpha_1^{m,n}}{2} + \cot\frac{\alpha_2^{m,n}}{2} + \cot\frac{\alpha_3^{m,n}}{2} - \frac{\mathcal{P}^2}{4\mathcal{A}},$$

$$f_3 := \frac{1}{\alpha_1^{m,n}} + \frac{1}{\alpha_2^{m,n}} + \frac{1}{\alpha_3^{m,n}} - \mathcal{R}.$$

  Take the initial guess $(\alpha_1, \alpha_2, \alpha_3)$ minimizing the residuals.

---

3   Numerical examples

In this section, we test the performance of our proposed reconstruction algorithm for three different triangles shown in Fig. 2.

3.1   Reconstruction of $\mathcal{A}, \mathcal{P}, \mathcal{R}$

At first, we test the algorithm for finding $\mathcal{A}, \mathcal{P}, \mathcal{R}$ from the spectral information through the heat trace by solving (2.4).

Example 3.1. We consider an isosceles right triangle, and set the length as 2 for the two edges sharing the right angle, cf. the left plot in Fig. 2. Then according to [16], the eigenvalues associated with the Dirichlet Laplacian take the form

$$\lambda = \left(\left(\frac{m}{2} \right)^2 + \left(\frac{n}{2} \right)^2 \right) \pi^2, \quad m,n = 1,2,\ldots, \quad m > n. \tag{3.1}$$

Note that in this example, we have the exact values of the area $\mathcal{A}$, perimeter $\mathcal{P}$, and $\mathcal{R}$

$$\mathcal{A} = 2, \quad \mathcal{P} = 4 + 2\sqrt{2} \approx 6.828427124746190, \quad \mathcal{R} = 10/\pi \approx 3.183098861837907.$$

In Table 1 we present the recovered $\mathcal{A}, \mathcal{P}$, and $\mathcal{R}$ with different numbers of eigenvalues (NoE) and $t_1 = 1.0e\text{-}3$, $t_2 = 1.0e\text{-}4$ and $t_3 = 1.0e\text{-}5$. We find that quite a lot of eigenvalues are necessary to reconstruct $\mathcal{A}, \mathcal{P}$, and $\mathcal{R}$ from the heat trace. Or else, as shown in Tables 1-3, we may obtain negative $\mathcal{A}, \mathcal{P}$, and $\mathcal{R}$ with a few eigenvalues, which is clearly not reasonable. In Tables 2 and 3 we set respectively $t_1 = 1.0e\text{-}2, t_2 = 1.0e\text{-}3, t_3 = 1.0e\text{-}4$ and $t_1 = 1.0e\text{-}2, t_2 = 2.0e\text{-}2, t_3 = 3.0e\text{-}2$. We observe that the number of eigenvalues is largely reduced when we increase t. This suggests that t should be not too small to ensure sufficient decay of the heat trace for large eigenvalues. However, t can also not be too large otherwise the asymptotic formula (2.1) does not hold. Our experience shows that the reconstruction algorithm has the best performance, i.e. least number of eigenvalues, when t is at the magnitude of 1.0e-2, as shown in Table 3. The number of required eigenvalues NoE=190 still seems to be somewhat large. It is of independent interest to further reduce such NoE by selecting an alternative set of parameters. However, this is beyond the scope of this paper.

From the observations, we always take $t_1 = 1.0e\text{-}2, t_2 = 2.0e\text{-}2$ and $t_3 = 3.0e\text{-}2$ in the subsequent numerical simulations.
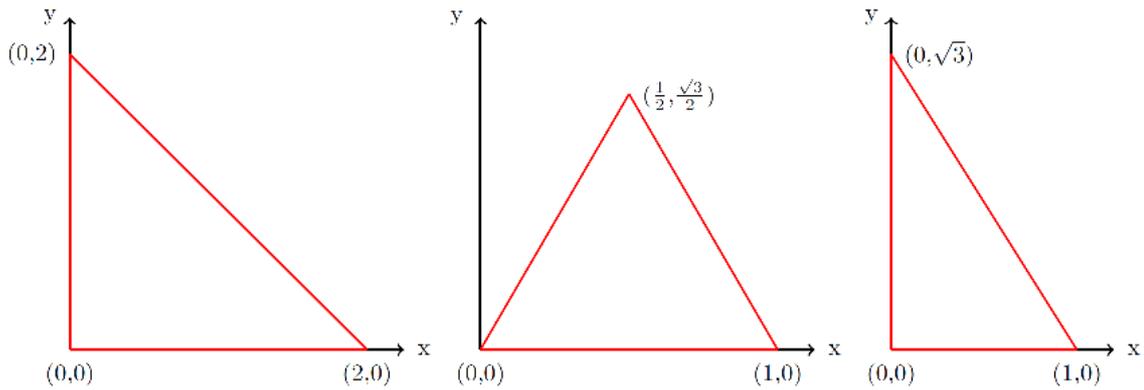

Figure 2: An illustration of the isosceles right triangle (left), the equilateral triangle (middle) and the right triangle with angles $(\pi/6, \pi/3, \pi/2)$ (right).

Table 1: Reconstructed $\mathcal{A}, \mathcal{P}$, and $\mathcal{R}$ from the heat trace for Example 3.1 with different NoE for $t_1 = 1.0\mathrm{e}\text{-}3$, $t_2 = 1.0\mathrm{e}\text{-}4$ and $t_3 = 1.0\mathrm{e}\text{-}5$.

NoE	$\mathcal{A}$	$\mathcal{P}$	$\mathcal{R}$
4950	-2.9129313603658291e-01	-3.1696515558990478e+02	-4.1203911743457111e+03
19900	1.0522528699226434e+00	-1.3392584266590384e+02	-1.8187045740588967e+03
44850	1.7785623564442550e+00	-2.6059580040879467e+01	-4.2251622064146892e+02
79800	1.9683097478176039e+00	2.1217782251929656e+00	-5.7739328693549737e+01
124750	1.9971602239092066e+00	6.4066624466044075e+00	-2.2761840796925257e+00
179700	1.9998405325710644e+00	6.8047429585942725e+00	2.8765332082378077e+00
244650	1.9999944160210454e+00	6.8275977899900031e+00	3.1723640296383020e+00
319600	1.9999998786233473e+00	6.8284090978635854e+00	3.1828655236329388e+00
404550	1.9999999983678343e+00	6.8284268823626162e+00	3.1830957245416860e+00
499500	1.9999999999863354e+00	6.8284271227429860e+00	3.1830988360029240e+00

Table 2: Reconstructed $\mathcal{A}, \mathcal{P}$, and $\mathcal{R}$ from the heat trace for Example 3.1 with different NoE for $t_1 = 1.0\mathrm{e}\text{-}2$, $t_2 = 1.0\mathrm{e}\text{-}3$ and $t_3 = 1.0\mathrm{e}\text{-}4$.

NoE	$\mathcal{A}$	$\mathcal{P}$	$\mathcal{R}$
4950	1.8374247413035629e+00	-8.0712701950282861e-01	-2.8070926390809980e+01
19900	1.9999457220428660e+00	6.8258778913407738e+00	3.1726642812281418e+00
44850	1.9999999998413398e+00	6.8284271172956741e+00	3.1830988313426598e+00
79800	1.9999999999998128e+00	6.8284271247385604e+00	3.1830988618080491e+00

Table 3: Reconstructed $\mathcal{A}, \mathcal{P}$, and $\mathcal{R}$ from the heat trace for Example 3.1 with different NoE for $t_1 = 1.0\mathrm{e}\text{-}2$, $t_2 = 2.0\mathrm{e}\text{-}2$ and $t_3 = 3.0\mathrm{e}\text{-}2$.

NoE	$\mathcal{A}$	$\mathcal{P}$	$\mathcal{R}$
45	1.4775748126505990e+00	-6.0740403397257000e-01	-9.3630927901357701e+00
190	1.9998516984964387e+00	6.8262777254156086e+00	3.1794182855915203e+00
435	1.9999999996677862e+00	6.8284271199313187e+00	3.1830988535931208e+00
780	2.0000000000000089e+00	6.8284271247464083e+00	3.1830988618384048e+00
1225	2.0000000000000089e+00	6.8284271247464083e+00	3.1830988618384048e+00

Example 3.2. We consider the equilateral triangle such that $0 < y < \sqrt{3}x$ and $y < \sqrt{3}(1-x)$, cf. the middle plot of Fig. 2. The eigenvalues are given by (cf. [20, 22])

$$\lambda = \frac{16\pi^2}{9}(m^2 + n^2 - mn), \quad m, n = 1, 2, \ldots, \quad m > n.$$

In the second example, we have the exact values of the area $\mathcal{A}$, the perimeter $\mathcal{P}$, and $\mathcal{R}$

$$\mathcal{A} = \sqrt{3}/4 \approx 0.433012701892219, \quad \mathcal{P} = 3, \quad \mathcal{R} = 9/\pi \approx 2.864788975654116.$$

In Table 4 we present the recovered $\mathcal{A}, \mathcal{P}$, and $\mathcal{R}$ with different NoE. Compared to Example 3.1, we can see that less eigenvalues are required to reconstruct $\mathcal{A}, \mathcal{P}$, and $\mathcal{R}$ from the heat trace.

Table 4: Reconstructed $\mathcal{A}, \mathcal{P}$, and $\mathcal{R}$ from the heat trace for Example 3.2 with different NoE for $t_1 = 1.0\text{e-}2$, $t_2 = 2.0\text{e-}2$ and $t_3 = 3.0\text{e-}2$.

NoE	$\mathcal{A}$	$\mathcal{P}$	$\mathcal{R}$
45	4.3301211487691948e-01	2.9999913010718919e+00	2.8647736791708787e+00
190	4.3301266184546344e-01	2.9999992285850343e+00	2.8647872541191282e+00
435	4.3301266184546344e-01	2.9999992285850343e+00	2.8647872541191282e+00
780	4.3301266184546344e-01	2.9999992285850343e+00	2.8647872541191282e+00
1225	4.3301266184546344e-01	2.9999992285850343e+00	2.8647872541191282e+00

Example 3.3. We consider a right triangle with angles $(\pi/6, \pi/3, \pi/2)$, and set the length as 2 for the longest edge, cf. the right plot in Fig. 2. Then according to [22], the eigenvalues associated with the Dirichlet Laplace take the form

$$\lambda = \frac{4\pi^2}{9}(m^2 + n^2 + mn), \quad m,n = 1,2,\ldots, \quad m > n.$$

In the third example, we have the exact values of the area $\mathcal{A}$, the perimeter $\mathcal{P}$, and $\mathcal{R}$

$$\mathcal{A} = \sqrt{3}/2 \approx 0.866025403784439,$$
$$\mathcal{P} = 3 + \sqrt{3} \approx 4.732050807568877,$$
$$\mathcal{R} = 11/\pi \approx 3.501408748021698.$$

In Table 5 we present the recovered $\mathcal{A}$, $\mathcal{P}$, and $\mathcal{R}$ with different NoE.

Table 5: Reconstructed $\mathcal{A}, \mathcal{P}$, and $\mathcal{R}$ from the heat trace for Example 3.3 with different NoE for $t_1 = 1.0\text{e-}2$, $t_2 = 2.0\text{e-}2$ and $t_3 = 3.0\text{e-}2$.

NoE	$\mathcal{A}$	$\mathcal{P}$	$\mathcal{R}$
45	8.5723629366654619e-01	4.6048114271670766e+00	3.2837299127641213e+00
190	8.6602540105196857e-01	4.7320507677516419e+00	3.5014086793903600e+00
435	8.6602540373955628e-01	4.7320508067043159e+00	3.5014087460923053e+00
780	8.6602540373955628e-01	4.7320508067043159e+00	3.5014087460923053e+00
1225	8.6602540373955628e-01	4.7320508067043159e+00	3.5014087460923053e+00

3.2 Reconstruction of the triangles

With the computed $\mathcal{A}, \mathcal{P}$, and $\mathcal{R}$ from the heat trace with 190 eigenvalues, our next step is to determine the triangles.

In the following triangle reconstructions, we consider the noisy eigenvalues in either the multiplicative form

$$\lambda_i^{\delta} := \lambda_i \left(1 + 2\delta\left(\texttt{rand}() - 0.5\right)\right)$$

or the additive form

$$\lambda_i^\delta := \lambda_i + 2\delta\big(\text{rand}() - 0.5\big),$$

where δ is the noisy level and $\text{rand}()$ is the built-in function of Matlab.

Fig. 3 shows the results for Example 3.1. The tolerance is 1.0e-6 for the Newton method and 2.0e-7 for the Levenberg-Marquardt algorithm for either the error between two consecutive iterations or for the residual of the nonlinear system of equations. We can observe very good reconstructions for the noise-free eigenvalues and the eigenvalues with small noise. However, when the noisy level for the multiplicative case increases to 1.0e-2, we can observe an obvious shift of the triangle. The additive case shows better results for the noise eigenvalues, this observation may be explained by the relatively larger values of the eigenvalues compared to the noise.

Fig. 4 shows the results for Example 3.2. In this case, our initial guess already gives a sufficient accurate solution for the noise-free case so that no Newton or Levenberg-Marquardt iterations are performed. For noisy data, since the Jacobian matrix is nearly singular, we use the Levenberg-Marquardt iterations. When $\delta = 1.0\text{e-}3$ we can still observe a very good reconstruction. However, the reconstruction quality deteriorates with increased noisy level for the multiplicative case. Similarly, the additive noise case gives better results.

(a) The multiplicative noise case: $\delta = 1.0\text{e-}3$ (left) and $\delta = 1.0\text{e-}2$ (right)

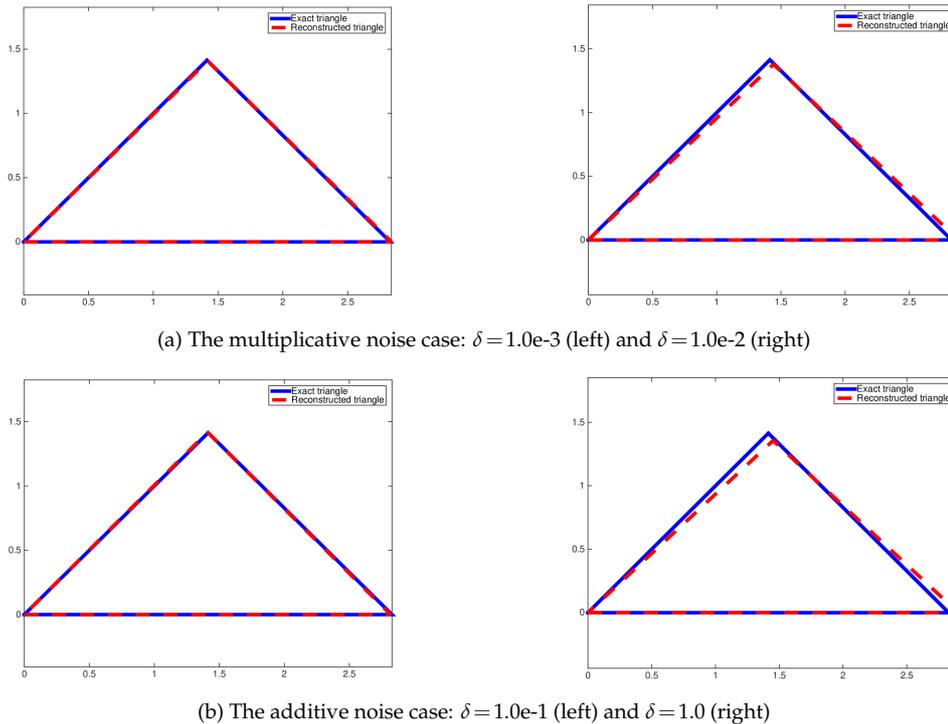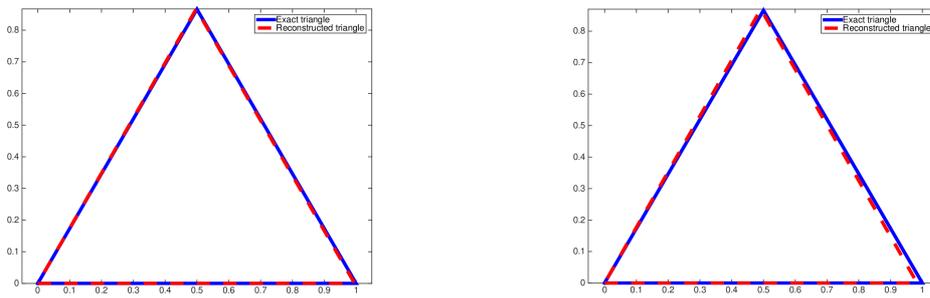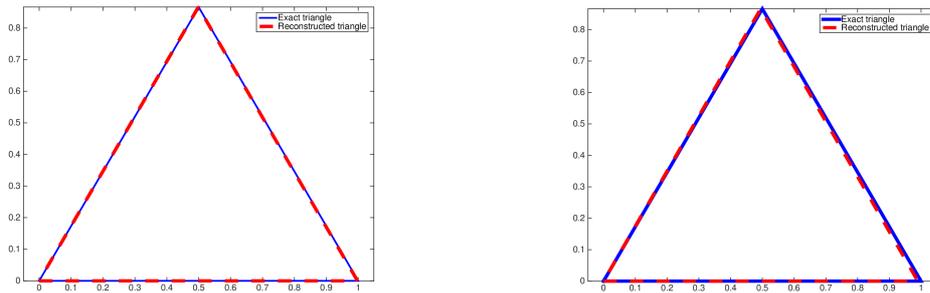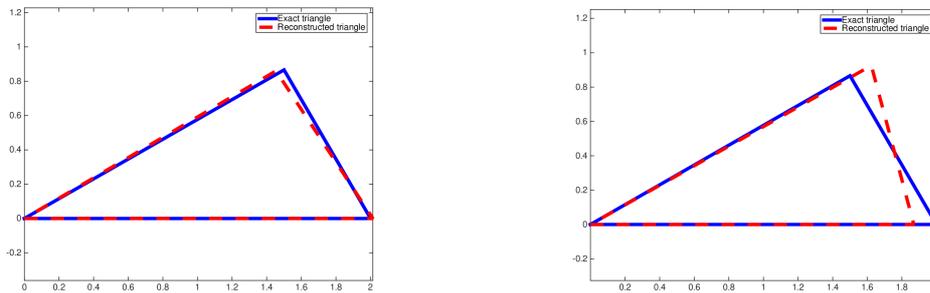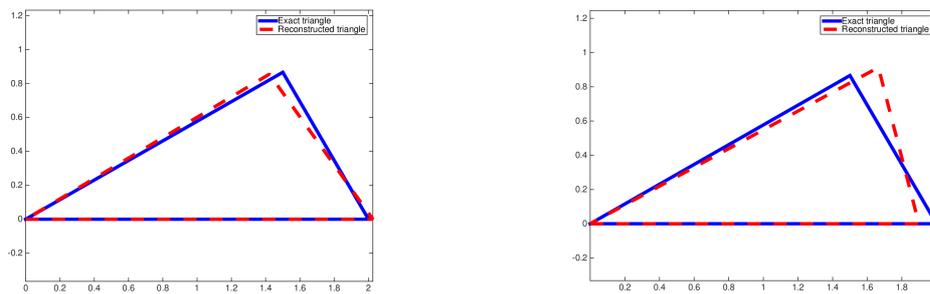(b) The additive noise case: $\delta = 1.0\text{e-}1$ (left) and $\delta = 1.0$ (right)

Figure 3: The comparisons of the exact and reconstructed triangles for Example 3.1 with noisy eigenvalues.

(a) The multiplicative noise case: $\delta = 1.0e\text{-}3$ (left) and $\delta = 1.0e\text{-}2$ (right)

(b) The additive noise case: $\delta = 1.0e\text{-}1$ (left) and $\delta = 1.0$ (right)

Figure 4: The comparisons of the exact and reconstructed triangles for Example 3.2.

(a) The multiplicative noise case: $\delta = 1.0e\text{-}3$ (left) and $\delta = 1.0e\text{-}2$ (right)

(b) The additive noise case: $\delta = 1.0e\text{-}2$ (left) and $\delta = 1.0e\text{-}1$ (right)

Figure 5: The comparisons of the exact and reconstructed triangles for Example 3.3.

Fig. 5 shows the results for Example 3.3. Similar reconstruction results are observed for noisy data. From this example, we also observe that the smallest angle has the best reconstruction. This may due to the fact that the Eqs. (2.6)-(2.7) are sensitive to the smallest angle.

Appendix A. Uniqueness and nonuniqueness for quadrilaterals based on symmetry

Theorem A.1. *Let the triangle $\mathcal{T}_{ABC}$, and the quadrilaterals $\mathcal{Q}_{AOBC}$ and $\mathcal{Q}_{ABCD}$ be defined in Fig. 6. Denote by $\{\lambda_n\}$ the Dirichlet eigenvalue set of $-\Delta$ for the triangle $\mathcal{T}_{ABC}$. Then all the eigenvalues λ_n are also the eigenvalues of $-\Delta$ both in the quadrilaterals $\mathcal{Q}_{AOBC}$ and $\mathcal{Q}_{ABCD}$.*
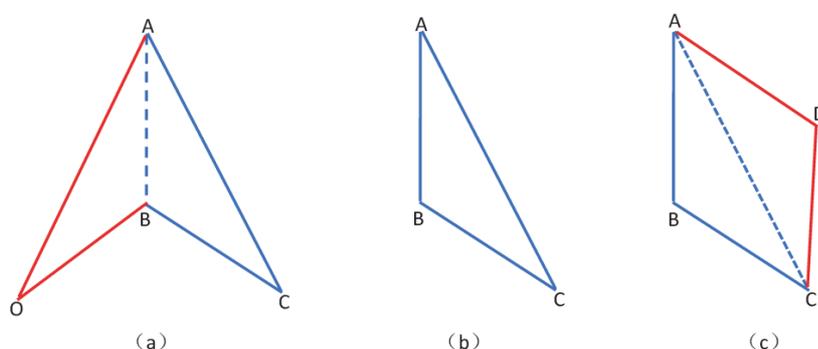

Figure 6: For a triangle $\mathcal{T}_{ABC}$ shown in (b), we have the quadrilaterals $\mathcal{Q}_{AOBC}$ and $\mathcal{Q}_{ABCD}$ as shown in (a) and (c), respectively, by folding the triangle $\mathcal{T}_{ABC}$ with respect to AB and AC.

Proof. We show that all the eigenvalues λ_n are the eigenvalues of $-\Delta$ in the quadrilateral $\mathcal{Q}_{AOBC}$. The case for the quadrilateral $\mathcal{Q}_{ABCD}$ follows similarly.

Denote by $\mathcal{R}_{AB}$ the reflection with respect to the line AB in $\mathbb{R}^2$. For each eigenvalue $\lambda \in \{\lambda_n\}$, let u be the corresponding eigenfunction defined in the triangle $\mathcal{T}_{ABC}$. Define

$$\begin{cases} u(x), & x \in \mathcal{T}_{ABC}, \\ -u(\mathcal{R}_{AB}x), & x \in \mathcal{T}_{AOB}. \end{cases}$$

Then we have

$$-\Delta v = \lambda v \quad \text{in } \mathcal{Q}_{AOBC},$$
$$v = 0 \qquad \text{on } \partial\mathcal{Q}_{AOBC} := AO \cup OB \cup BC \cup CA.$$

This completes the proof.   □

The above theorem shows that the two different quadrilaterals $\mathcal{Q}_{AOBC}$ and $\mathcal{Q}_{ABCD}$ share infinitely many eigenvalues. Conversely, even if we have infinitely many eigenvalues, the shape of a quadrilateral may not be heard.

Theorem A.2. *A parallelogram can be heard from the corresponding spectrum.*

Proof. This has been proved by Lu and Rowlett recently in [18]. Here, we give a slight different proof, which may seem to be simpler. Firstly, the asymptotic behavior (2.1) implies that the area $\mathcal{A}$, the perimeter $\mathcal{P}$, and the sum $\mathcal{R}$ of the reciprocals of the angles of the parallelogram can be heard from all the spectrum. Secondly, using the notations shown in Fig. 7,

$$\mathcal{A} = pq\sin\alpha, \tag{A.1}$$

$$\mathcal{P} = 2(p+q), \tag{A.2}$$

$$\mathcal{R} = \frac{2}{\alpha} + \frac{2}{\pi-\alpha}, \tag{A.3}$$

where $\alpha \in (0, \pi/2]$.

By (A.3), we find that α is the small root of the quadratic equation

$$\mathcal{R}x^2 - \pi\mathcal{R}x + 2\pi = 0.$$

Furthermore, insert α into (A.1), from (A.1)-(A.2), we deduce that the adjacent sides p and q are roots of the quadratic equation

$$x^2 - \frac{\mathcal{P}}{2}x + \frac{\mathcal{A}}{\sin\alpha} = 0.$$

In a sum, with the help of the heat trace, the eigenvalues uniquely determine three parameters $\mathcal{A}, \mathcal{P}, \mathcal{R}$, from which the adjacent sides p, q and angle α are uniquely determined. Obviously, a parallelogram is uniquely determined by the adjacent sides p, q and angle α. The proof is complete. $\square$
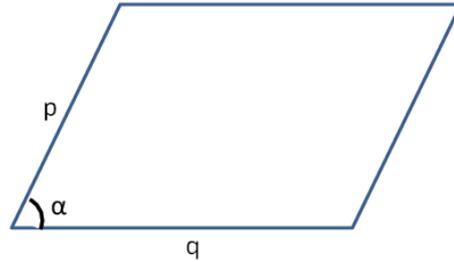

Figure 7: A parallelogram whose adjacent sides are p and q with angle α.

Acknowledgments

References

[1] P. R. S. Antunes and P. Freitas, *New bounds for the principal Dirichlet eigenvalue of planar regions*, Exp. Math., 15(3):333–342, 2006.

[2] P. R. S. Antunes and P. Freitas, *A numerical study of the spectral gap*, J. Phys. A Math. Theor., 41(5):055201, 2008.

[3] P. R. S. Antunes and P. Freitas, *On the inverse spectral problem for Euclidean triangles*, Proc. R. Soc. A., 467(2130):1546–1562, 2011.

[4] M. van den Berg and S. Srisatkunarajah, *Heat equation for a region in $\mathbb{R}^2$ with a polygonal boundary*, J. Lond. Math. Soc. (2), 37(1):119–127, 1988.

[5] P.-K. Chang and D. DeTurck, *On hearing the shape of a triangle*, Proc. Amer. Math. Soc., 105(4):1033–1038, 1989.

[6] J. De Simoi, V. Kaloshin, and Q. Wei, *Dynamical spectral rigidity among $\mathbb{Z}_2$-symmetric strictly convex domains close to a circle*, Ann. Math., 186(1):277–314, 2017.

[7] C. Durso, *On the Inverse Spectral Problem for Polygonal Domains*, PhD Thesis, Massachusetts Institute of Technology, 1990.

[8] J. Fan and Y. Yuan, *On the quadratic convergence of the Levenberg-Marquardt method without nonsingularity assumption*, Computing, 74(1):23–39, 2005.

[9] J. Gómez-Serrano and G. Orriols, *Any three eigenvalues do not determine a triangle*, J. Differential Equations, 275:920–938, 2021.

[10] C. Gordon, D. Webb, and S. Wolpert, *Isospectral plane domains and surfaces via Riemannian orbifolds*, Invent. Math., 110:1–22, 1992.

[11] D. S. Grebenkov and B.-T. Nguyen, *Geometrical structure of Laplacian eigenfunctions*, SIAM Review, 55(4):601–667, 2013.

[12] D. Grieser and S. Maronna, *Hearing the shape of a triangle*, Notices Amer. Math. Soc., 60(11):1440–1447, 2013.

[13] H. Hezari, Z. Lu, and J. Rowlett, *The Dirichlet isospectral problem for trapezoids*, J. Math. Phys., 62(5):051511, 2021.

[14] H. Hezari and S. Zelditch, *One can hear the shape of ellipses of small eccentricity*, Ann. of Math. (2), 196(3):1083–1134, 2022.

[15] M. Kac, *Can one hear the shape of a drum?* Amer. Math. Monthly, 73:1–23, 1966.

[16] J. R. Kuttler and V. G. Sigillito, *Eigenvalues of the Laplacian in two dimensions*, SIAM Review, 26(2):163–193, 1984.

[17] R. S. Laugesen and B. A. Siudeja, *Triangles and other special domains*, in: A. Henrot. Shape Optimization and Spectral Theory, De Gruyter Open, 159–200, 2017.

[18] Z. Lu and J. Rowlett, *The sound of symmetry*, Amer. Math. Monthly, 122(9):815–835, 2015.

[19] H. P. McKean Jr. and I. M. Singer, *Curvature and the eigenvalues of the Laplacian*, J. Differential Geom., 1(1):43–69, 1967.

[20] M. A. Pinsky, *The eigenvalues of an equilateral triangle*, SIAM J. Math. Anal., 11(5):819–827, 1980.

[21] B. A. Siudeja, *Sharp bounds for eigenvalues of triangles*, Michigan Math. J., 55:243–254, 2007.

[22] J. C. Sun, *Pre-transformed methods for eigen-problems II: Eigen-structure for Laplace eigen-problem over arbitrary triangles*, Math. Numer. Sin., 34(1):1–24, 2012.

[23] S. Zelditch, *Inverse spectral problem for analytic domains II: $\mathbb{Z}_2$-symmetric domains*, Ann. Math., 170(1):205–269, 2009.